

Pulmonary histopathological findings of COVID-19

Hallazgos histopatológicos pulmonares de COVID-19

César Luna-Rivero*, Tania Pérez-Marmolejo, Francina V. Bolaños-Morales, Armando Castorena-Maldonado, Arturo I. González-González, and Jesús A. Rivero-Martínez

Departamento de Patología, Instituto Nacional de Enfermedades Respiratorias Ismael Cosío Villegas, Mexico City, Mexico

Abstract

Since the beginning of the COVID-19 pandemic, three clinical stages of disease severity have been described. All these stages manifest with diverse clinical scenarios, ranging from an asymptomatic form to a severe form characterized by acute respiratory distress syndrome with multiple organ dysfunction. At least three primary histological patterns of lung injury have been recorded: 1) epithelial pattern, characterized by diffuse alveolar damage with varying degrees of organization, denudation, hyperplasia of pneumocytes, as well as possible cytopathic changes; 2) vascular pattern, characterized by diffuse intra-alveolar fibrin and/or the presence of microvascular thrombi (fibrin); and 3) fibrotic pattern, which includes fibrotic diffuse alveolar damage and/or interstitial fibrosis. In this study, we describe the post-mortem histopathological findings of COVID-19, including our experience at the INER with 40 patients, 28 men and 12 women. The most frequent patterns were acute alveolar damage ($n = 23$), chronic cellular infiltrate ($n = 10$), and minimal change pattern ($n = 7$). The fibrotic pattern was found in 38 patients, involving $< 20\%$; the alveolar filling pattern was described in all patients, in $< 30\%$ of the tissue; and the nodular pattern was present in 7 patients, in $< 10\%$ of the tissue. The connection between these pathological findings and the clinical course of COVID-19 suggests the possibility that pathogenesis follows a sequential pattern. In the initial phase of viral infection, respiratory epithelial cells become infected; therefore, epithelial changes predominate with evidence of viral activity.

Keywords: Morphological changes. COVID-19. Autopsy. SARS-CoV-2.

Resumen

Desde el inicio de la pandemia se describieron tres etapas clínicas de gravedad de la COVID-19. Estas etapas de la enfermedad se manifiestan con escenarios clínicos diversos, desde una forma asintomática hasta una forma grave caracterizada por síndrome de insuficiencia respiratoria aguda con disfunción orgánica múltiple. Se han registrado al menos tres patrones histológicos primarios de lesión pulmonar: 1) patrón epitelial, caracterizado por daño alveolar difuso con diversos grados de organización, denudación e hiperplasia de neumocitos, así como posibles cambios citopáticos; 2) patrón vascular, caracterizado por fibrina intraalveolar difusa o presencia de trombos microvasculares (fibrina); y 3) patrón fibrótico, que incluye daño alveolar difuso fibrótico o fibrosis intersticial. En este trabajo describimos los hallazgos histopatológicos post mortem en pacientes con COVID-19 e incluimos la experiencia del INER con 40 pacientes (28 hombres y 12 mujeres). Los patrones más frecuentes fueron daño alveolar agudo ($n = 23$), infiltrado celular crónico ($n = 10$) y patrón de cambios mínimos ($n = 7$). El patrón de fibrosis se encontró en 38 pacientes, con afectación $< 20\%$; el patrón de llenado alveolar fue descrito en todos

*Correspondence:

César Luna-Rivero
E-mail: lunarivero@hotmail.com

Date of reception: 05-11-2025
Date of acceptance: 07-11-2025
DOI: 10.24875/NCTE.M26000019

Available online: 12-05-2026
Neumol Cir Torax (Eng). 2025;84(2):128-136
www.revistanct.org.mx

2594-1526 / © 2025 Sociedad Mexicana de Neumología y Cirugía de Tórax. Publicado por Permanyer. Este es un artículo open access bajo la licencia CC BY-NC-ND (<http://creativecommons.org/licenses/by-nc-nd/4.0/>).

los pacientes, en < 30% de la pieza; y el patrón nodular estuvo presente en 7 pacientes, en < 10% de la pieza. La conexión entre estos hallazgos patológicos y el curso clínico de la COVID-19 indica la posibilidad de que la patogenia siga un patrón secuencial. En la fase inicial de la infección viral, las células epiteliales respiratorias se infectan y, por tanto, predominan los cambios epiteliales con evidencia de actividad viral.

Palabras clave: Cambios morfológicos. COVID-19. Autopsia. SARS-CoV-2.

Introduction

On December 31st, 2019, Chinese health authorities reported 27 cases of acute respiratory syndrome of unknown etiology in Wuhan. A novel coronavirus, severe acute respiratory syndrome coronavirus 2 (SARS-CoV-2), was subsequently identified as the causative agent. The disease rapidly spread worldwide. In Mexico, the first confirmed case was reported on February 27, 2020, and on March 11 the World Health Organization declared coronavirus disease 2019 (COVID-19) a global pandemic.

Since the beginning of the pandemic, 3 clinical stages of disease severity have been described. The initial stage is characterized by SARS-CoV-2 infection, with symptoms such as rhinorrhea, headache, and malaise, similar to those of a common cold. The second stage is characterized by pulmonary inflammation and coagulopathy, which may develop consecutively or overlap, with elevation of inflammatory biomarkers such as C-reactive protein, ferritin, interleukin (IL)-6, IL-1, and D-dimer; these findings are associated with the development of acute respiratory distress syndrome (ARDS) and a worse prognosis. Finally, the third stage is characterized by fibrosis. All these stages may present with diverse clinical scenarios, ranging from asymptomatic infection to severe disease characterized by ARDS with multiorgan dysfunction. During the pandemic, COVID-19 mortality was 5.4%; however, comorbidities, including diabetes mellitus and arterial hypertension, as well as advanced age, substantially increased mortality^{1,2}.

Although numerous studies have reported epidemiologic data, clinical characteristics, and potential treatments for COVID-19, pathologic reports have been less frequent, limiting comprehensive understanding of disease progression and outcomes³. A major limitation for such studies was the risk associated with tissue sampling, making biosafety a critical concern. The Royal College of Pathologists published biosafety guidelines for postmortem studies in individuals with SARS-CoV-2 infection to reduce the risk of viral transmission⁴.

Histopathologic findings

Case series describing histopathologic findings have focused primarily on pulmonary lesions at different stages, including hyaline membrane formation, type II pneumocyte hyperplasia, and the presence of thrombi and fibrin in small arterial vessels, consistent with coagulopathy⁵. At least 3 primary histologic patterns of lung injury have been described: (1) an epithelial pattern, characterized by diffuse alveolar damage (DAD) with varying degrees of organization, denudation, and pneumocyte hyperplasia, with possible cytopathic changes; (2) a vascular pattern, characterized by diffuse intra-alveolar fibrin or microvascular thrombi (fibrin); and (3) a fibrotic pattern, including fibrotic DAD or interstitial fibrosis.

According to Katzenstein and Askin⁶, DAD is a nonspecific pulmonary reaction to multiple injurious agents. The common denominator is endothelial and alveolar injury leading to exudation of fluids and cells, which may progress to extensive interstitial pulmonary fibrosis. The most characteristic pathologic finding in the acute stage of DAD is the presence of hyaline membranes, which appear on light microscopy as homogeneous, eosinophilic material lining the inner surface of the alveoli. Hyaline membranes consist of necrotic epithelial cell debris and serum proteins that have leaked from the circulation into the alveolar space due to increased permeability of the alveolocapillary barrier. The appearance of DAD depends on the time elapsed between exposure to the injurious factor and histologic examination. Three consecutive phases are recognized: an early (exudative) phase characterized by intra-alveolar exudate, hyaline membranes, and cellular infiltrate predominantly composed of lymphocytes, plasma cells, and macrophages; an intermediate (proliferative) phase characterized by hyperplasia, atypia, and mitoses of type II pneumocytes with thrombosis of small pulmonary arteries; and a late (fibrotic or organizing) phase characterized by thickening of the alveolocapillary membrane, fibroblast proliferation (particularly in the interstitium), and fibrosis. In severe cases, fibrosis may progress within weeks, restructuring the entire

Table 1. Pulmonary histopathologic patterns identified in severe COVID-19

Histologic pattern	Elements of the pattern
1. Diffuse alveolar damage (DAD)	Acute intra-alveolar exudate with partial filling of alveolar spaces, hyaline membrane formation, granulation tissue deposition, and fibroblast proliferation
2. Fibrosis	Replacement of the interstitium by fibrous tissue characterized by excessive accumulation of extracellular matrix components, predominantly collagen
3. Chronic inflammatory infiltrate	Interstitial widening due to proliferation predominantly of lymphocytes and plasma cells
4. Alveolar filling pattern	Complete or near-complete occupation of alveolar spaces by cellular elements (macrophages, lymphocytes, neutrophils) and noncellular components (fibrin and cellular debris)
5. Nodular pattern	One or multiple nodules of varying size and shape; a distinct interface between the nodular lesion and adjacent normal lung parenchyma is observed
6. Minimal changes	Largely preserved alveolar architecture on low-power microscopy ($\times 4$); however, high-power examination ($\times 40$) reveals multifocal injury involving alveolar walls, interstitium, small airways, and blood vessels

pulmonary parenchyma and producing a honeycomb lung pattern with near-complete replacement of the alveolar space. Different phases may overlap, and multiple evolutionary stages may be observed in the same patient⁷.

A systematic review by Polak et al.⁷ showed that some pulmonary histopathologic findings differ significantly between COVID-19 and conventional ARDS or other forms of viral pneumonitis. Typical ARDS findings include acute interstitial pneumonia with edema and DAD of varying degrees of organization⁸. Influenza pneumonitis often shows capillary and small-vessel thrombosis, interstitial edema, neutrophilic and lymphoplasmacytic interstitial inflammatory infiltrates, hyaline membrane formation, varying degrees of intra-alveolar edema or hemorrhage, and acute DAD, as well as necrotizing bronchitis and bronchiolitis. Later stages include organizing DAD, fibrosis, epithelial regeneration, and squamous metaplasia⁷. In other coronavirus infections, such as Middle East respiratory syndrome and the prior severe acute respiratory syndrome caused by SARS-CoV, patients develop small airway obstruction due to airway denudation, inflammatory cell infiltrates, hemorrhage, alveolar edema, and hyaline membrane formation – features typical of the exudative phase of DAD.⁹ In contrast, COVID-19-related pneumonitis appears to encompass epithelial, vascular, and fibrotic patterns of lung injury¹⁰.

When histopathologic patterns are analyzed according to time from symptom onset, some studies suggest a relatively clear timeline. Epithelial changes, including DAD, denudation, and reactive pneumocyte atypia, were present at almost all stages. Vascular changes,

including microvascular injury, thrombi, intra-alveolar fibrin deposition, and other features of acute fibrinous and organizing pneumonia, also occurred during early symptomatic infection¹⁰. This vascular injury pattern appears more prominent in COVID-19 than in conventional ARDS or influenza and is consistent with clinical studies reporting thrombotic events in up to 49% of cases. This finding correlates with expression of the angiotensin-converting enzyme 2 (ACE2) receptor in both alveolar epithelium and capillary endothelium. On the other hand, interstitial fibrotic changes generally appeared several weeks after symptom onset, although some patients showed early fibrosis, likely attributable to preexisting lung disease rather than SARS-CoV-2 infection.

Other studies have examined correlations among ventilatory parameters, computed tomography findings, and histologic patterns. Chest computed tomography typically demonstrated multiple bilateral ground-glass opacities or consolidation. Laboratory studies showed normal leukocyte counts in most patients, frequent lymphopenia, and elevated inflammatory biomarkers, including C-reactive protein, D-dimer, and creatine kinase¹¹. These findings have contributed to understanding the multisystem behavior of the virus.

As an emerging disease, COVID-19 pathophysiology is not yet fully understood. Postmortem studies may improve understanding and help refine therapeutic strategies. Because the literature on histopathologic changes in patients infected with SARS-CoV-2 remains limited, we aimed to analyze, describe, and correlate histopathologic findings with clinical, biochemical, and radiologic evolution in patients who died during the COVID-19 pandemic

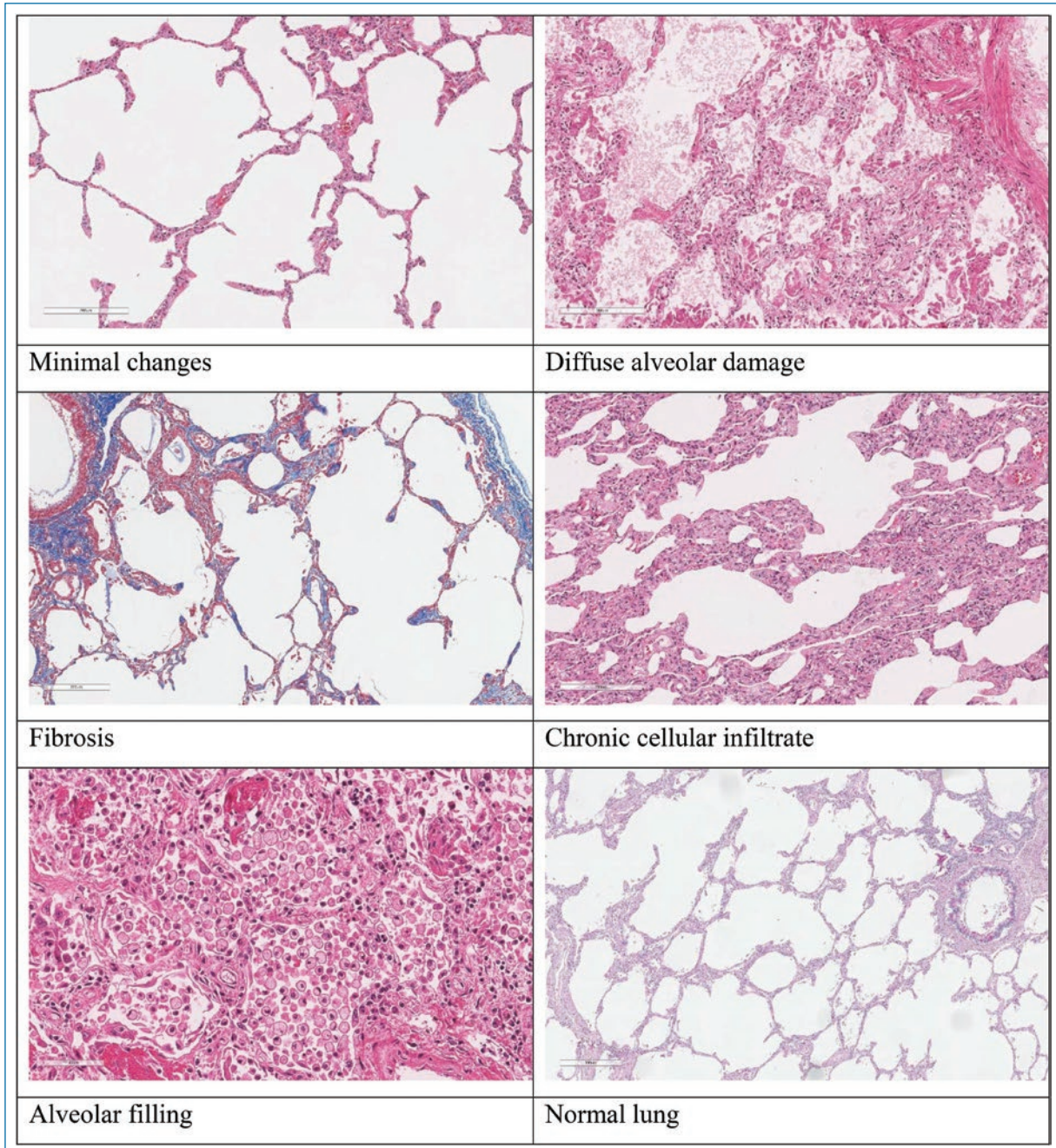


Figure 1. Representative images of pulmonary morphologic patterns in patients with severe COVID-19.

at Instituto Nacional de Enfermedades Respiratorias Ismael Cosío Villegas (INER).

The INER experience

Postmortem histopathologic findings were available for 40 patients (28 men and 12 women) with a mean (SD, 12.6) age of 55.4 years. Regarding comorbidities, 8 patients (20%) had hypertension, 1 (2.5%) had ischemic

heart disease, 1 (2.5%) had chronic kidney disease requiring hemodialysis, 25 (62.5%) had varying degrees of obesity, 15 (37.5%) had a history of chronic alcohol use, and 8 (20%) had chronic obstructive pulmonary disease (COPD). All patients were symptomatic. The mean duration of symptoms prior to admission was 8.5 days (95% CI, 6.75-15), and the mean length of stay, 11 days (95% CI, 6.75-15.25). At admission, all patients had clinical features (dyspnea, cough, myalgias, fatigue,

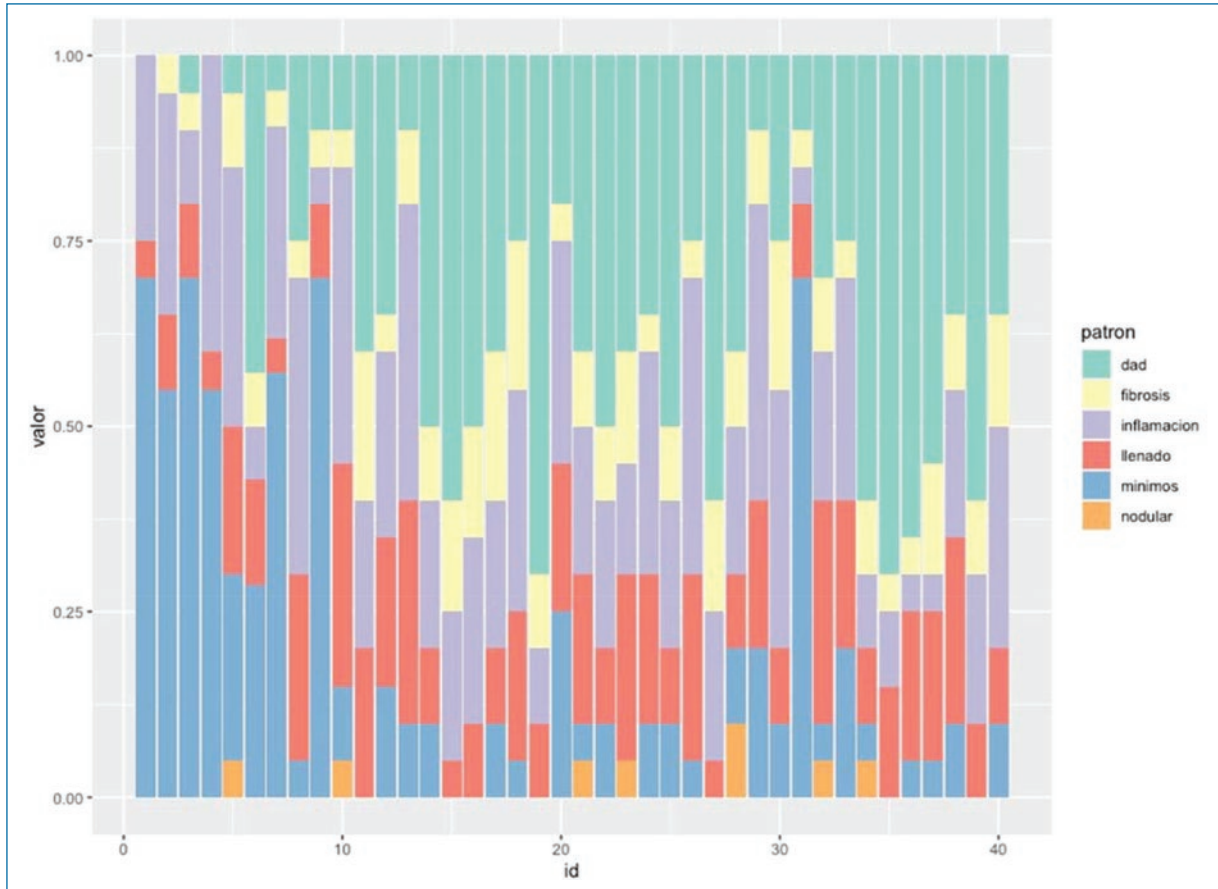


Figure 2. Graphic distribution of pulmonary histopathologic patterns in 40 patients who died from severe COVID-19.

Table 2. Clinical characteristics of patients according to the predominant histologic pattern of lung injury

Characteristic	All (n = 40)	Histologic pattern			p
		Acute lung injury pattern (n = 23)	Chronic inflammatory infiltrate (n = 10)	Minimal changes (n = 7)	
Age, years	55.4 (12.6)	55.2 (11.7)	59.4 (14.7)	50.4 (3.2)	0.50
Sex, M/F, No., n (%)	28/12 (70/30)	17/6 (74/26)	6/4 (60/40)	5/2 (71/29)	0.80
Comorbidities					
Diabetes	14 (35)	8 (57.1)	4 (28.6)	2 (14.3)	1.00
Hypertension	8 (20)	11 (68.8)	3 (18.8)	2 (12.5)	0.50
Cardiovascular disease	1 (2.5)	-	-	-	-
COPD	8 (20)	4 (50)	1 (12.5)	3 (37.5)	0.30
Chronic kidney disease	1 (2.5)	0	1 (100)	0	0.43
Obesity	25 (62.5)	16 (64.4)	5 (20)	4 (16)	0.60
Alcohol use disorder	15 (37.5)	8 (53.3)	4 (26.6)	3 (20)	1.00

(Continue)

Table 2. Clinical characteristics of patients according to the predominant histologic pattern of lung injury (*continuation*)

Characteristic	All (n = 40)	Histologic pattern			p
		Acute lung injury pattern (n = 23)	Chronic inflammatory infiltrate (n = 10)	Minimal changes (n = 7)	
Symptoms					
Cough	26 (65)	13 (50)	6 (23.1)	7 (26.9)	0.09
Myalgia or fatigue	25 (62.5)	14 (56)	7 (28)	4 (16)	0.80
Headache	13 (32.5)	6 (46.2)	4 (30.8)	3 (23.1)	0.59
Diarrhea	4 (10)	2 (50)	0	2 (50)	0.18
Dyspnea	36 (90)	20 (55.6)	9 (25)	7 (19.4)	1.00
Fever	37 (92.5)	21 (56.8)	9 (24.3)	7 (18.9)	1.00
Anosmia	5 (12.5)	3 (60)	2 (40)	0	0.68
Dysgeusia	10 (25)	7 (70)	2 (20)	1 (10)	0.69
SpO ₂ , mean (SD)	82.5 (12.6)	84.6 (11.8)	75.8 (14.2)	85.1 (10.8)	0.15
PaO ₂ /FiO ₂ , median (IQR)	130 (97-165)	129 (98-148)	150 (100-162)	130 (82-176)	0.63

Data are presented as No. (%) unless otherwise indicated. SpO₂ values are expressed as mean (SD), and PaO₂/FiO₂ as median (interquartile range). COPD: chronic obstructive pulmonary disease; FiO₂: fraction of inspired oxygen; PaO₂: arterial oxygen partial pressure; SpO₂: oxygen saturation.

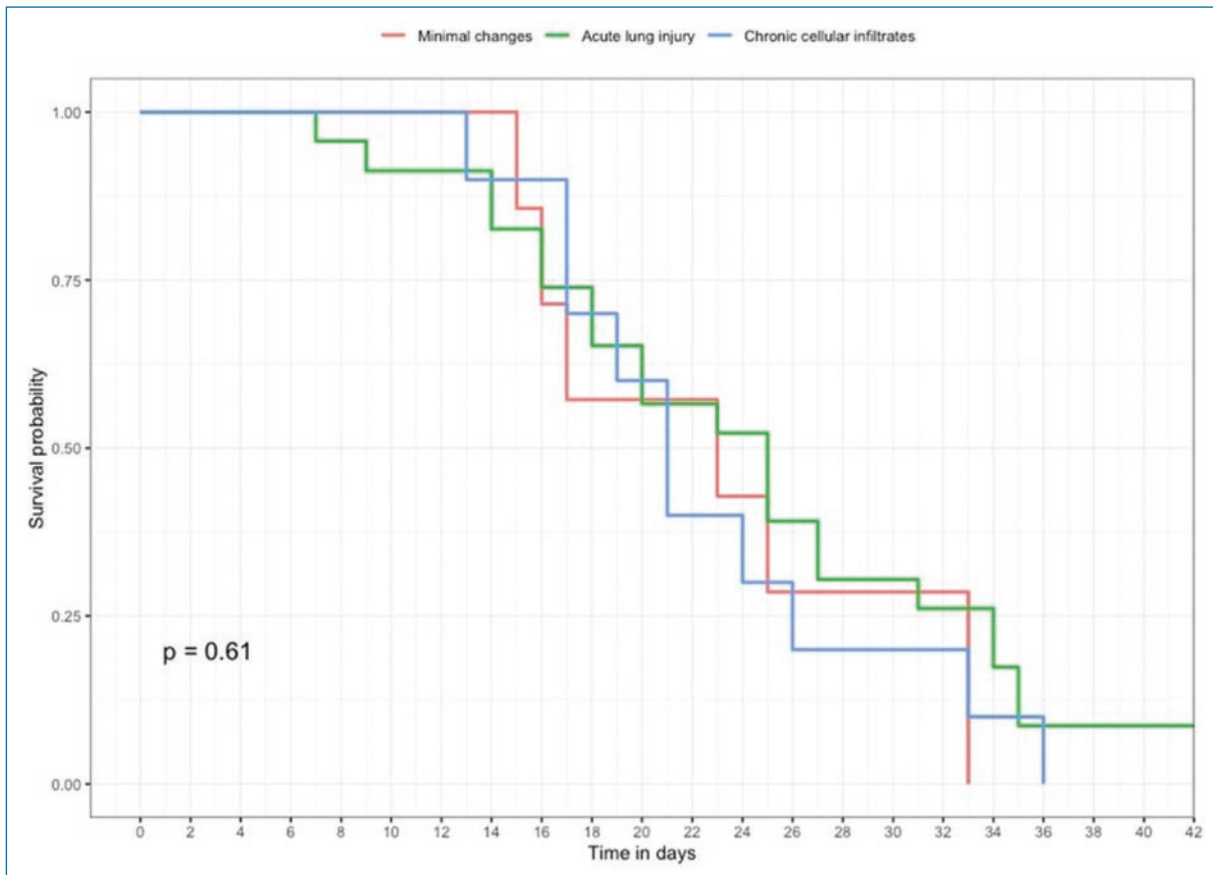


Figure 3. Kaplan-Meier survival curves of patients who died from severe COVID-19, according to predominant histologic pattern.

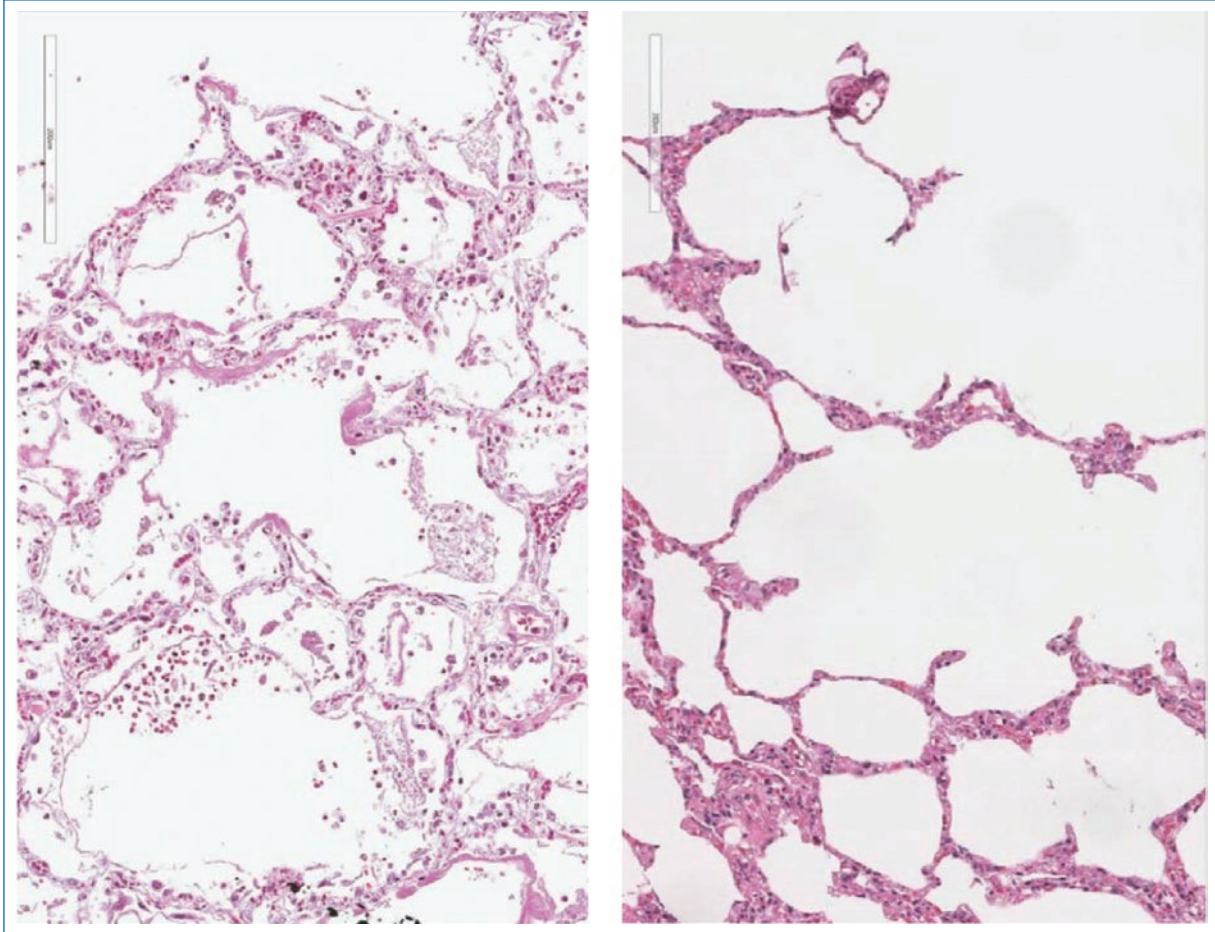


Figure 4. Comparison of histologic findings in influenza H1N1 and COVID-19. The left panel shows a photomicrograph of lung tissue affected by influenza H1N1, demonstrating diffuse alveolar damage with hyaline membrane formation and intra-alveolar granulation tissue, without significant interstitial or microvascular injury (hematoxylin-eosin stain, original magnification $\times 20$). The right panel shows lung tissue affected by COVID-19, with alveolar wall injury characterized by pneumonitis and microvascular obstruction due to fibrin microthrombi (hematoxylin-eosin stain, original magnification $\times 20$).

headache, fever, anosmia, dysgeusia, and diarrhea) and radiologic findings consistent with interstitial pneumonia, classified into 3 tomographic stages according to progression. Mean oxygen saturation at hospital admission was 82% (SD, 12.5), with a mean $\text{PaO}_2/\text{FiO}_2$ ratio of 130 (95% CI, 97-164). Mechanical ventilation was required in 39 patients, with a median duration of 11.5 days (95% CI, 8.25-17). During hospitalization, non-existent acute kidney injury at admission developed in 27 patients (67.5%). Secondary infection was documented in 19 patients (47.5%), including *Pseudomonas* (n = 5), *Acinetobacter* (n = 5), *Klebsiella* (n = 3), *Staphylococcus* (n = 3), and *Candida* (n = 3). Regarding treatment, 17 patients received ritonavir and oseltamivir; 23 (57.5%) received antibiotics of various classes; 21 (52.2%) received hydroxychloroquine; and

5 (12.5%) received tocilizumab. Methylprednisolone was administered in 25 patients (62.5%), and 34 (85%) required vasopressors during hospitalization.

Table 1 and figure 1 illustrate the 6 histologic patterns identified on microscopic examination of lung tissue. For each case, the predominant pattern was recorded, although most specimens showed a combination of patterns (Figure 2). The most frequent predominant patterns were acute alveolar damage (DAD) (n = 23), chronic inflammatory infiltrate (n = 10), and minimal changes (n = 7). A fibrotic pattern was present in 38 patients, affecting less than 20% of the specimen. An alveolar filling pattern was observed in all patients, involving < 30% of the tissue. A nodular pattern was identified in 7 patients, affecting less than 10% of the specimen. Table 2 presents clinical parameters

according to the predominant histologic pattern of lung injury.

No statistically significant associations were identified between clinical variables and predominant histologic patterns. However, DAD was the most frequent pattern in patients with greater comorbidity burden. These patients had a higher number of symptoms at admission and lower oxygen saturation in the chronic inflammatory infiltrate group, although differences among the 3 groups were not statistically significant (Table 2). Patients in the DAD group required longer durations of mechanical ventilation and more frequently developed acute kidney injury and secondary infections; however, no significant differences were observed regarding specific pharmacologic interventions. Kaplan-Meier survival curves according to predominant histologic pattern are shown in figure 3; no statistically significant differences were found. A combination of 6 characteristic histologic patterns was observed in all specimens, with predominance of DAD. The proportion of DAD increased over time during the pandemic and according to the timing of biopsy acquisition, possibly reflecting the progression of the pandemic and the use of multiple therapeutic strategies.

Histopathologic findings in influenza pneumonitis often include capillary and small-vessel thrombosis, interstitial edema, neutrophilic and lymphoplasmacytic interstitial inflammatory infiltrates, hyaline membrane formation, varying degrees of intra-alveolar edema or hemorrhage, and acute DAD, in addition to necrotizing bronchitis and bronchiolitis (Figure 4). Later stages include organizing DAD, fibrosis, epithelial regeneration, and squamous metaplasia. In other coronavirus infections, such as Middle East respiratory syndrome and prior severe acute respiratory syndrome caused by SARS-CoV, patients develop small airway obstruction due to airway denudation, along with inflammatory cell infiltrates, hemorrhage, alveolar edema, and hyaline membrane formation – typical features of the exudative phase of DAD. In our series, airway denudation was not a characteristic finding. Vascular damage in COVID-19–related lung damage was frequently identified in the specimens, compared with conventional ARDS and influenza. In multiple studies, this vascular injury has been associated with the presence of the ACE2 receptor in both alveolar epithelium and capillary endothelium. Fibrotic changes have been described after 3 weeks from symptom onset; although fibrosis was present in 38 patients from the beginning of the pandemic in our series, it was not the predominant pattern. This finding may be related to preexisting COPD.

Final considerations

The association between pathologic findings and the clinical course of COVID-19 suggests that pathogenesis may follow a sequential pattern. In the early phase of viral infection, respiratory epithelial cells are infected, and epithelial changes with evidence of viral activity predominate. Subsequent viral clearance appears reduced in patients with severe disease or underlying risk factors. The presence of epithelial lung injury with hyperplasia, pneumocyte atypia, and multinucleation – possibly reflecting viral cytopathic effects – even in later stages of COVID-19, supports this hypothesis. Based on our findings in the INER population, we consider that COVID-19 may present with overlapping or sequential stages.

Funding

The authors declare that no funding was received.

Conflicts of interest

The authors declared no conflicts of interest whatsoever.

Ethical considerations

Protection of persons and animals. The authors declare that no experiments were performed on humans or animals for this research.

Confidentiality, informed consent, and ethical approval. The study does not involve personal patient data and did not require ethics committee approval. SAGER guidelines do not apply.

Declaration on the use of artificial intelligence. The authors declare that no generative artificial intelligence tools were used in the preparation of this manuscript.

References

1. Organización Panamericana de la Salud y Organización Mundial de la Salud. Alerta epidemiológica: nuevo coronavirus (nCoV). 16 de enero de 2020, Washington, D.C.: OPS/OMS; 2020.
2. Li B, Yang J, Zhao F, Zhi L, Wang X, Liu L, et al. Prevalence and impact of cardiovascular metabolic diseases on COVID-19 in China. *Clin Res Cardiol.* 2020;109:531-8. <https://doi.org/10.1007/s00392-020-01626-9>.
3. Farver CF, Zander DS. Molecular basis of pulmonary disease. En: Coleman WB, Tsongalis GJ, editores. *Molecular pathology.* Philadelphia: Elsevier; 2009. p. 305-64. Available from: <https://pmc.ncbi.nlm.nih.gov/articles/PMC7158196/pdf/main.pdf>.
4. Osborn M, Lucas S, Stewart R, Swift B, Youd E. Autopsy practice relating to possible cases of COVID-19 (2019-nCoV, novel coronavirus from China 2019/2020) secondary autopsy practice relating to possible cases of COVID-19. Royal College of Pathologists; 2020. Available in: <https://www.rcpath.org/static/d5e28baf-5789-4b0f-acecfe370eee6223/fe8fa85a-f004-4a0c-81ee4b2b9cd12cbf/Briefing-on-COVID-19-autopsy-Feb-2020.pdf>.

5. Sharma A, Tiwari S, Deb MK, Marty JL. Severe acute respiratory syndrome coronavirus-2 (SARS-CoV-2): a global pandemic and treatment strategies. *Int J Antimicrob Agents*. 2020;56:106054. <https://doi.org/10.1016/j.ijantimicag.2020.106054>.
6. Katzenstein AA, Askin FB. Surgical pathology of non-neoplastic lung disease. *Major Probl Pathol*. 1982;13:1-430.
7. Polak SB, Van Gool IC, Cohen D, von der Thüsen JH, van Paassen J. A systematic review of pathological findings in COVID-19: a pathophysiological timeline and possible mechanisms of disease progression. *Mod Pathol*. 2020;33:2128-38. <https://doi.org/10.1038/s41379-020-0603-3>.
8. Narasaraju T, Yang E, Samy RP, Ng HH, Poh WP, Liew AA, et al. Excessive neutrophils and neutrophil extracellular traps contribute to acute lung injury of influenza pneumonitis. *Am J Pathol*. 2011;179:199-210. <https://doi.org/10.1016/j.ajpath.2011.03.013>.
9. Lim AYH, Goh JL, Chua MCW, Heng BH, Abisheganaden JA, George PP. Temporal changes of haematological and radiological findings of the COVID-19 infection-a review of literature. *BMC Pulm Med*. 2021;21:37. <https://doi.org/10.1186/s12890-020-01389-z>.
10. Barth RF, Buja LM, Barth AL, Carpenter DE, Parwani AV. A comparison of the clinical, viral, pathologic, and immunologic features of Severe Acute Respiratory Syndrome (SARS), Middle East Respiratory Syndrome (MERS), and coronavirus 2019 (COVID-19) diseases. *Arch Pathol Lab Med*. 2021;145:1194-211. <https://doi.org/10.5858/arpa.2020-0820-sa>.
11. Onishi Y, Kawamura T, Higashino T, Mimura R, Tsukamoto H, Sasaki S. Clinical features of acute fibrinous and organizing pneumonia: an early histologic pattern of various acute inflammatory lung diseases. *PLoS One*. 2021;16:e0249300. <https://doi.org/10.1371/journal.pone.0249300>.